Raman microprobe analysis during the direct laser writing of silicon microstructures

Frank Magnotta and Irving P. Herman
Department of Physics, University of California Lawrence Livermore National Laboratory, Livermore, California 94550

(Received 19 August 1985; accepted for publication 6 November 1985)

Raman microprobe techniques are used for the first time as a real-time probe during local direct laser writing and also as an *in situ* probe after writing. The Stokes–Raman emission observed during pyrolytic deposition of micron-dimension structures of silicon on germanium and vitreous carbon substrates is found to be weaker, more asymmetric, and to peak at a smaller Raman shift than the corresponding spectrum of the same structure similarly probed *in situ* after deposition. Results of detailed post-deposition Raman analysis of these silicon microstructures are presented and compared to the Raman spectra of oven-heated silicon. Potential applications of these techniques are discussed.

Direct laser writing of micron-dimension semiconductor and metal interconnection structures is of potential use for repair and semicustomization of integrated circuits and for other microelectronics applications.[1–3] In most studies of local deposition performed to date, the only real-time, *in situ* diagnostics have been visual inspection through a microscope and measurement of substrate optical reflection and transmission. Quite often, neither of these techniques is versatile enough to provide information suitable for process control or elucidating the kinetics of deposition. Raman scattering at low laser intensity has proven to be a powerful tool for nonperturbative characterization of semiconductors, in some cases with micron resolution. This letter reports the first use of Raman microprobe techniques as a real-time probe during direct laser writing and also as an *in situ* probe after direct laser writing. In this study undoped silicon microstructures were deposited by a pyrolytic process[4,5] and analyzed with the Raman technique.

Raman scattering is a sensitive probe of local silicon properties, such as temperature,[6–10] stress,[11,12] crystallinity,[11,13] and morphology,[14] each of which is important in this work. The temperature dependence of Raman scattering in silicon has been previously investigated in detail using both conventional oven heating[6,7] and focused laser heating.[6,8–10]

In the experimental apparatus an argon-ion laser (5145 Å) was directed to and focused onto a substrate as described in previous reports[2]; a vidicon permitted on-line viewing. The focused laser induces pyrolytic microdeposition of silicon from silane by local heating of the substrate and also provides photons for the spontaneous Raman spectrum. The substrate was housed in a reaction chamber which was mounted on a motor-driven *x-y* stage and plumbed to a gas manifold/vacuum system by a set of bellows. Backscattered Raman radiation was collected and collimated by the focusing objective, and was directed to the detection system, consisting of a set of four interference filters to prefilter out 5145 Å, a 1-m single monochrometer, and a cooled, microchannel plate intensified, diode array rapid scanning spectrometer/signal averager.

The polycrystalline Ge and vitreous carbon substrates used in this study were degreased by rinsing with standard solvents prior to introduction into the reaction vessel and subsequent bake-out and pump-down. SiH_4 (99.99%) was purified by freeze-pump-thaw cycles (77 K) to remove volatiles before filling the reaction cell (100–700 Torr).

Figure 1, trace (a) depicts a typical Stokes–Raman spectrum obtained during the laser deposition of a silicon line ($\sim 5\,\mu$m wide, $\sim 1\,\mu$m high) on a germanium substrate, with an incident laser power of 700 mW and beam radius of about 2 μm, 350 Torr SiH_4, and a cell scanning speed of $\sim$0.1 mm/s. Characteristically these real-time spectra have a large, broad, asymmetric profile peaking near 486 cm^{-1} representing the leading edge of the scanning reaction zone for silicon deposition. In the experimental regimes under examination silicon deposition occurred only with laser intensities high enough to locally melt the germanium substrate ($T_{mp} = 1210$ K).

After the silicon line depicted in Fig. 1 trace (a) was written, the gas in the cell was evacuated and replaced with an equal pressure of xenon buffer gas to ensure the same scanning characteristics of the cell. The laser then retraced this line at the same laser power and focus, and scan speed,

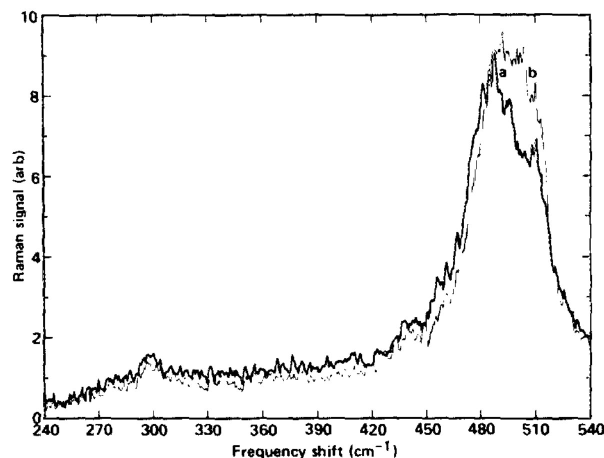

FIG. 1. Raman spectra obtained during direct laser writing (trace a, bold line) and during *in situ* reading (trace b, thin line) of silicon on germanium for 700 mW of 5145 Å focused to a $\sim 2\,\mu$m beam radius, 350 Torr SiH_4, and a $\sim$0.1 mm/s scanning speed. The small peak at 300 cm^{-1} is from the germanium substrate.

Downloaded 22 Jul 2008 to 128.59.65.82. Redistribution subject to AIP license or copyright; see http://apl.aip.org/apl/copyright.jsp

producing trace (b) in Fig. 1. This trace is very nearly symmetric and peaks near 493 cm^{-1}. The real-time "writing" Stokes spectrum (trace a) is smaller (by ~10% in integrated signal), more asymmetric, and has a slightly smaller Raman frequency displacement compared to the post-deposition "reading" peak (trace b). These novel features and differences are even more pronounced for silicon deposition on vitreous carbon, for which the integrated "writing" signal is 20–40% smaller than that measured during post-deposition "reading."

The position of the scanning focused laser defines the leading edge of the deposited line and the site of Raman scattering. Within this leading region of deposition the thickness of the silicon deposit increases from nearly zero to nearly the final silicon line thickness. If the film is thinner than the laser absorption depth over significant portions of this reaction zone, then for equal temperatures the integrated intensity of the Stokes peak during the writing cycle will be smaller than during the reading cycle, as seen in Fig. 1. For the 5145-Å beam probing silicon, this absorption depth is about 0.2 μm at 1000 K.[15]

The asymmetry of the real-time Raman peak suggests that the probed region consists of silicon with sharply varying local properties, such as temperature, strain, crystallinity, and phase. During writing and also reading at high laser power, elastically backscattered light exhibited a swirling pattern, suggesting that the silicon was partially molten. Nemanich *et al.*[16] found that molten silicon has a "featureless" Raman profile, while at the melting point (1690 K) *c*-Si shows a peak at 480 cm^{-1}, with a 30-cm^{-1} width. Therefore, the weaker signal observed here during the write cycle could also be due to a larger molten phase during writing than during reading. The real-time "writing" peak at 486 cm^{-1} is 6 cm^{-1} higher in frequency than the *c*-Si Raman peak at melting, and would imply a 1500-K temperature if it represented uniformly heated silicon.[6] However, because of Raman averaging arising from local temperature inhomogeneities during deposition (see below), this spectral peak suggests that the deposit may be molten or near melting during writing.

A possible explanation for the slightly smaller Stokes shift observed during the writing step is that the local temperature is greater during writing than during the post-deposition read, though the laser conditions are the same in both cases. Heat can be conducted away from the reaction zone during writing by the germanium substrate and the effectively semi-infinite silicon line already written; whereas during most of a read cycle heat conduction occurs to the substrate and the effectively infinitely long (on both sides) silicon line, leading to a lower temperature during reading than during writing.[17] This effect is even more pronounced when writing on a thermal insulator, such as vitreous carbon.[17] Heat supplied to the reaction zone due to the surface deposition reaction is much smaller than that supplied by the laser.

Following the same experimental procedure as outlined above, several other silicon lines were written on germanium and then read afterwards. In some cases, the laser power used to read was successively decreased from the power used during deposition to 1–10 mW. The data from one such run are reproduced in Fig. 2(a). The Raman peaks show a monotonically increasing width, decreasing Raman shift, increasing flattening of the peak (i.e., deviation from Lorentzian behavior), increasing "noise," and slightly increasing asymmetry (increasingly larger low-frequency tails) with increasing laser intensity. Alternately, in some runs the laser power was increased from low values to that used during writing. There was no significant difference in the data obtained using either procedure, suggesting that any laser annealing during the reading cycles does not substantially affect the observations. In either case the Raman shift and width of these written polycrystalline silicon lines were 519 and 4.3 cm^{-1}, respectively, at low laser power, which are very close to the corresponding values for crystalline silicon measured here, 520 and 3.4 cm^{-1}. (Deconvolution of the 2.2-cm^{-1} instrumental linewidth gives 3.7 cm^{-1} for the laser-written lines and 2.6 cm^{-1} for the crystalline silicon linewidths.) Since the coefficient of thermal expansion of

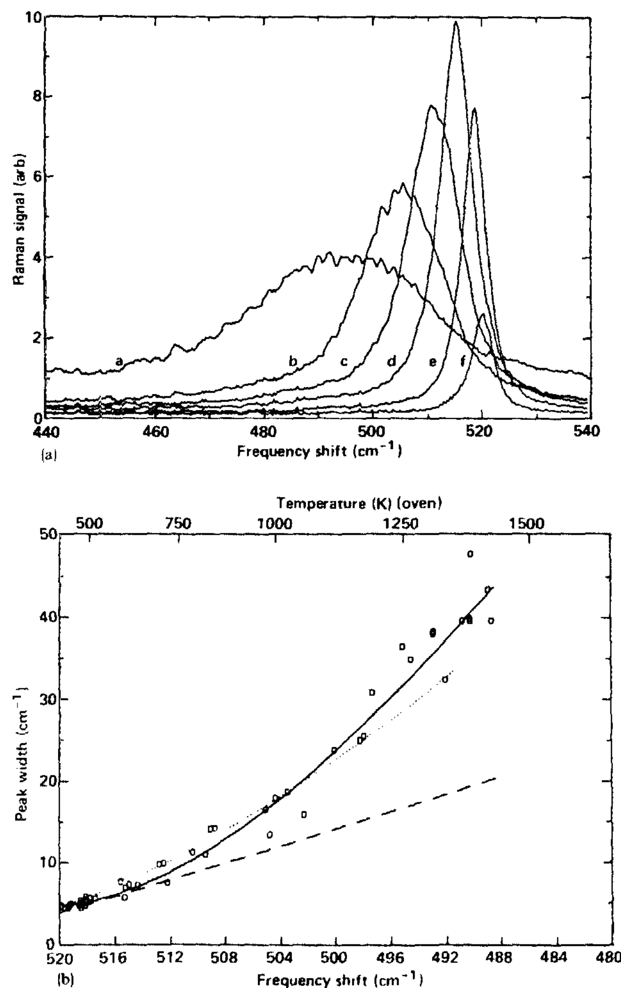

FIG. 2. (a) Post-deposition Raman spectra of a previously deposited silicon microstructure on germanium. Incident laser powers are a: 725 mW, b: 500 mW, c: 375 mW, d: 250 mW, e: 100 mW, f: 25 mW. (b) Raman frequency shifts plotted vs peak width (FWHM; not deconvoluted for instrumental linewidth). Post-deposition data from several runs using germanium substrates are shown, along with a solid line fit. The dashed line shows a fit to the Raman results for oven-heated silicon from Ref. 6; the corresponding temperature for the *oven* case is plotted as the top abscissa. The results of Ref. 6 have been extrapolated to 1450 K, beyond their temperature limit of 1200 K.[16] Also plotted for reference is the width/shift relation for the calculated spatially averaged Raman spectrum (dotted line; to 1690 K).

Downloaded 22 Jul 2008 to 128.59.65.82. Redistribution subject to AIP license or copyright; see http://apl.aip.org/apl/copyright.jsp

germanium exceeds that of silicon, a compressive stress and a corresponding slight increase in the Raman shift vis-à-vis crystalline silicon is expected; this is not seen here.

Figure 2(b) plots the peak widths as a function of Raman shifts of the run depicted in Fig. 2(a) and four other similar runs, with a solid line fit to the data. Also plotted in this figure is the FWHM width of the Raman signal versus the Raman frequency shift for silicon uniformly heated in an oven, obtained by Balkanski *et al.*[6] (dashed line). The top abscissa axis plots the oven temperature for the corresponding frequency shift of uniformly heated Si. For low laser powers, the results obtained here are quite close to the oven values; the local $-\delta(\text{width})/\delta(\text{shift})$ slope is about 0.65 compared to a fairly temperature-independent value of 0.50 for the oven results. The spectra obtained at higher laser power have widths much greater than expected from the corresponding oven results, as evidenced by a differential slope of about 1.8. Disparities with the oven results arise from the need to spatially sum the contributions from different regions in the focused laser case due to varying incident photon fluxes, temperature-dependent widths and Raman shifts, and strain. For comparison purposes, the width/shift relation for the spatially averaged Raman spectra is displayed in Fig. 2(b) (dotted line). It is derived from the thermal profiles provided in Ref. 17 for a locally heated deposit with thermal conductivity approximately twice that of the substrate (as for Si on Ge).[18] This curve ends where the peak temperature of the deposit is at melting (1690 K), whereas the (dashed) curve representing the case of uniform temperature ends at 1450 K.

The width/shift relation for silicon microstructures on vitreous carbon is similar to Fig. 2(b), though the corresponding laser powers employed were about 10 times smaller because of the lower thermal conductivity of the substrate. These observations suggest that Raman profile broadening due to phonon interactions with photoexcited carriers[9] (which would be approximately linear with laser power) is probably not significant here.

For comparison, the Raman spectrum from focused laser-heated crystalline silicon in a xenon ambient was also examined here. The Raman peaks were highly skewed to low frequencies,[8,10] and were much broader for a given Raman shift [corresponding to a slope of 4 in Fig. 2(b)] than for either the laser-fabricated and laser-heated microstructures or oven-heated silicon, in agreement with the calculations of spatially averaged Raman profiles.[18] Laser-heated microstructures exhibit narrower Raman spectra because they have flatter thermal profiles (when on substrates with lower thermal conductivity), have contributions from the regions most uniform in temperature due to the limited size of the deposit, and have less strain than do laser-heated substrates.

Recent measurements by Compaan and Trodahl[7] on oven-heated silicon show that as the temperature increases from 300 to 1000 K the Stokes scattering rate for a 5145-Å pump laser decreases monotonically by a factor of 2.5. In post-deposition reading of the silicon lines on germanium in this study, the integrated Raman signal normalized by the incident photon flux decreases about threefold as the incident power is increased from about 25 (sample near 298 K) to 800 mW. This is consistent with a maximum temperature during high-power reading greatly exceeding 1000 K.

This study suggests that, depending on the desired scan speeds and microstructure dimensions, Raman techniques are potentially useful for process control during writing (in real time) or after processing (*in situ*) for pyrolytic or photolytic deposition and etching of materials with strong first order Raman signals, such as silicon, germanium, III-V compounds, and metal silicides. Analysis of the spatially averaged Raman signal during processing can be used as a temperature monitor, either by using the breadth and shift of the Stokes line[18] or the Stokes/anti-Stokes intensity ratio. Use of a second laser as a Raman probe, perhaps at a different wavelength and with lower power and focused at or near the writing laser focus, can make this technique even more versatile.

Local temperatures near melting have been inferred from the Raman spectra during writing and high-power reading of silicon lines. A more quantitative comparison of the writing and reading spectra based on a model of the scanning reaction zone is under way. Also, studies of local germanium-silicon alloy fabrication and detection using these methods are in progress.

The authors wish to thank S. A. Letts for the loan of the scanning diode spectrometer and F. P. Milanovich for the loan of some spectral filtering equipment. This work was performed under the auspices of the U. S. Department of Energy by the Lawrence Livermore National Laboratory under contract number W-7405-ENG-48.

[1] I. P. Herman, in *Laser Processing and Diagnostics—Chemical Physics*, edited by D. Bauerle (Springer, New York, 1984), Vol. 39, 396.

[2] B. M. McWilliams, I. P. Herman, F. Mitlitsky, R. A. Hyde, and L. L. Wood, Appl. Phys. Lett. **43**, 946 (1983).

[3] D. J. Ehrlich and J. Y. Tsao, in *VLSI Electronics: Microstructure Science*, edited by N. Einspruch (Academic, New York, 1984), Vol. 7, p. 129.

[4] D. J. Ehrlich, R. M. Osgood, Jr., and T. F. Deutsch, Appl. Phys. Lett. **39**, 957 (1981).

[5] D. Bauerle, P. Irsigler, G. Leyendecker, H. Noll, and D. Wagner, Appl. Phys. Lett. **40**, 819 (1982).

[6] M. Balkanski, R. F. Wallis, and E. Haro, Phys. Rev. B **28**, 1928 (1983).

[7] A. Compaan and H. J. Trodahl, Phys. Rev. B **29**, 793 (1984).

[8] H. W. Lo and A. Compaan, J. Appl. Phys. **51**, 1565 (1980).

[9] D. Kirillov and J. L. Merz, in *Laser Diagnostics and Photochemical Processing for Semiconductor Devices-Materials Research Society Symposia Proceeding*, edited by R. M. Osgood, S. R. J. Brueck, and H. R. Schlossberg (North-Holland, New York, 1983), Vol. 17, p. 95.

[10] J. Raptis, E. Liarokapis, and E. Anastassakis, Appl. Phys. Lett. **44**, 125 (1984).

[11] D. V. Murphy and S. R. J. Brueck, in *Laser Diagnostics and Photochemical Processing for Semiconductor Devices—Materials Research Society Symposia Proceedings*, edited by R. M. Osgood, S. R. J. Brueck, and H. R. Schlossberg (North-Holland, New York, 1983), Vol. 17, p. 81 (and references cited therein).

[12] P. Zorabedian and F. Adar, Appl. Phys. Lett. **43**, 177 (1983).

[13] J. B. Hopkins, L. A. Farrow, and G. J. Fisanick, Appl. Phys. Lett. **44**, 535 (1984).

[14] D. V. Murphy and S. R. J. Brueck, Opt. Lett. **8**, 494 (1983).

[15] G. E. Jellison, Jr. and F. A. Modine, Appl. Phys. Lett. **41**, 180 (1982).

[16] R. J. Nemanich, D. K. Biegelsen, R. A. Street, and L. E. Fennel, Phys. Rev. B **29**, 6005 (1984).

[17] K. Piglmayer, J. Doppelbauer, and D. Bauerle, in *Laser-Controlled Chemical Processing of Surfaces—Materials Research Society Symposia Proceedings*, edited by A. W. Johnson, D. J. Ehrlich, and H. R. Schlossberg (North-Holland, New York, 1984), Vol. 29, p. 47.

[18] I. P. Herman and F. Magnotta (unpublished results).

Downloaded 22 Jul 2008 to 128.59.65.221. Redistribution subject to AIP license or copyright; see http://apl.aip.org/apl/copyright.jsp